



Cite this: DOI: 10.1039/c7nj02015e

Influence of the first and second coordination spheres on the diverse phenoxazinone synthase activity of cobalt complexes derived from a tetradentate Schiff base ligand†

Anangamohan Panja, *^a Narayan Ch. Jana^a and Paula Brandão^b

This paper describes syntheses and structural characterization of four new cobalt(III) compounds (**1–4**) derived from a N₃O donor Schiff base ligand, a condensation product of *N,N*-dimethyldipropylenetriamine and *o*-vanillin, and their catalytic activity relating to the function of phenoxazinone synthase. X-ray crystallography reveals that the Schiff base can coordinate the metal centre either in a tetradentate fashion through the monoanionic deprotonated form using all four donor sites (in **1** and **2**) or in a tridentate fashion using the zwitterionic form of the Schiff base ligand, leaving the quaternary amine nitrogen free from coordination (in **3**). The monoanionic deprotonated ligand can also bind the metal centre in a tridentate fashion where the pendent tertiary amine nitrogen is engaged in intramolecular hydrogen bonding in **4**. Moreover, the triamine part of the Schiff base ligand can bind a metal centre both facially and meridionally. Therefore, all these versatilities associated with this triamine make it appealing for the development of coordination chemistry with diverse structures. All complexes are active functional models for phenoxazinone synthase, and as expected the availability of labile sites at the first coordination sphere for the substrate, *o*-aminophenol, binding is responsible for higher catalytic activity in **1** and **2**. The importance of a proton abstraction site at the second coordination sphere behind the facile oxidation of the substrate is also explored (reactivity of **3** vs. **4**). The remarkable finding from the mass spectral study discloses several important intermediates, and thereby provides significant information relating to the mechanistic pathway of the functioning phenoxazinone synthase activity of the synthetic models.

Received 6th June 2017,
Accepted 31st July 2017

DOI: 10.1039/c7nj02015e

rsc.li/njc

Introduction

Oxidation reactions play an important role in the synthesis of valuable organic compounds, namely pharmaceuticals, agrochemicals, and other fine chemicals.^{1,2} Continuous pressure from society demands the adaptation of sustainable and environmentally benign processes in industrial synthesis by the replacement of traditional oxidants which are toxic and causing environmental pollution. Today, there is an increasing demand for the selective oxidation of organic compounds utilizing dioxygen as a primary oxidant for industrial application because of its economic and environmental benefits. However, the direct oxidation of organic substrates by molecular oxygen is rare because of its kinetic inertness, which is associated with the

triplet ground state of O₂; this high-energy barrier is nature's way of protecting organic compounds (typically in the singlet ground state) from destructive oxidation.^{3–6} Nature has also developed elegant mechanisms to make controlled aerobic oxidations under ambient conditions in which metalloenzymes activate molecular dioxygen and thereby facilitate the spin forbidden interaction between dioxygen and organic matter for biochemical oxidation processes.^{7–9} Bioinorganic chemists have made much effort to investigate enzyme active-site chemistry by the use of a synthetic analogue approach.^{10–12} These enzymatic models can furnish reference compounds to get insight into the structures of active sites and reactive intermediates and the mechanistic details of dioxygen activation and oxidation reactions occurring at the active sites.^{13–19} This type of information and insight is often not available from direct enzymatic studies. Moreover, highly efficient biomimetic models may provide new reagents or efficient catalysts for the alternative of traditional toxic inorganic (mostly heavy metals) catalysts for industrial processes. It is to be noted that the extraordinary catalytic activity of metalloenzymes is mainly associated with the crucial role of protein chains that help in substrate recognition and stabilisation

^a Postgraduate Department of Chemistry, Panskura Banamali College, Panskura RS, WB 721152, India. E-mail: ampanja@yahoo.co.in

^b Department of Chemistry, CICECO-Aveiro Institute of Materials, University of Aveiro, 3810-193 Aveiro, Portugal

† Electronic supplementary information (ESI) available: Fig. S1–S6. CCDC 1543047–1543050 for **1–4**. For ESI and crystallographic data in CIF or other electronic format see DOI: 10.1039/c7nj02015e

of the intermediate through various noncovalent forces.^{20–22} Therefore, development of synthetic analogues beyond the first coordination sphere could be the right way to develop efficient biomimetic catalysts.

We have been developing biomimetic catalysts for the oxidation of 3,5-di-*tert*-butylcatechol and *o*-aminophenol by molecular dioxygen, mimicking the function of catechol oxidase.^{23–25} and phenoxazinone synthase,^{26,27} respectively. The latter, a multi-copper metalloenzyme, catalyses the oxidative coupling of a wide variety of substituted *o*-aminophenols to phenoxazinone chromophores through catalytic activation of dioxygen in the final step for the biosynthesis of actinomycin D,²⁸ which is used clinically for the treatment of many tumours, including Wilm's tumour, where the phenoxazinone chromophore intercalates with DNA base-pairs, thereby strongly inhibiting DNA dependent RNA synthesis.^{29,30} From the active site structures of several oxidase enzymes and from the reports in the literature on various model complexes with transition metals,^{23–28,31–39} it is clear that the active site of the functional models must have labile or free coordination sites available for substrate binding. Therefore, the ligands having a lower number of donor atoms are more promising. Coordination compounds derived from the Schiff base ligands have been extensively studied as enzymatic models mainly because of their synthetic simplicity and tremendous structural diversities, and thereby fine tuning of the catalytic activity can be carried out by modification of the coordination environment at the metal centre by judicious choice of amine and carbonyl parts of the Schiff bases.

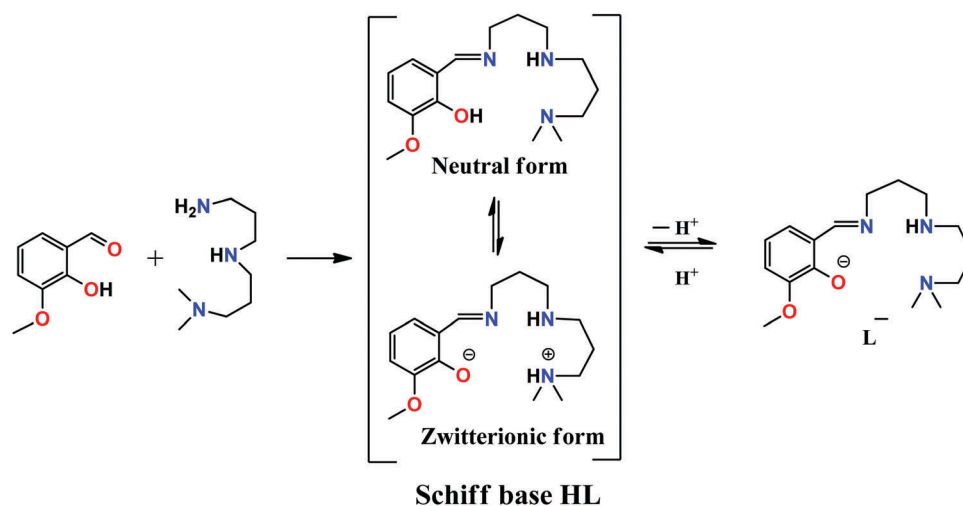
A triamine protected at one end, namely *N,N*-dimethyldipropylenetriamine, may produce N₄ or N₃O donor Schiff base ligands by reacting with pyridine-2-aldehyde or salicylaldehyde, respectively, for the development of coordination compounds having either vacant or labile position(s) available for substrate binding. Moreover, the presence of bis(propylene) linkers in this amine may increase the flexibility of the ligands so that substrate binding to the metal centre becomes possible. Furthermore, such ligands including several functions, namely

amine (both secondary and tertiary), imine, pyridine (from pyridine-2-aldehyde part) or phenol (from salicylaldehyde part), are able to provide different donor sites allowing fine tuning of the ligand field around the metal centre, and thereby may lead to significant improvement in the catalytic activity. Surprisingly, only single report on Cu(II) complexes with a Schiff base derived from *N,N*-dimethyldipropylenetriamine is available in the literature.⁴⁰ Therefore, we are interested in the systematic development of coordination chemistry of the transition metals derived from this triamine, with the goal of their potential applications in diverse fields, such as magnetic materials⁴¹ and biorelevant catalysis. Accordingly, in this present endeavour, Schiff base HL (Scheme 1) derived from *N,N*-dimethyldipropylenetriamine and *o*-vanillin was used for the synthesis of cobalt complexes in the presence of pseudohalides (azide, thiocyanate and cyanate). In continuation of our long-standing interest in the field of bioinspired catalysis,^{23–27} herein, we report the synthesis and structures of four new cobalt complexes, [Co(L)(N₃)₂].0.5CH₃CN (1), [Co(L)(NCS)₂].0.5H₂O (2), [Co(HL)₂][Co(NCS)₄].NCS (3) and [Co(L)₂]₂[Co(NCO)₄] (4), derived from Schiff base ligand HL and pseudohalides, and their biomimetic catalytic activity related to the function of phenoxazinone synthase. Interestingly, the influence of solvents and pseudohalides on the diverse coordination chemistry of cobalt was observed. Moreover, the different donor properties of the Schiff base associated with *N,N*-dimethyldipropylenetriamine part were also explored. Furthermore, emphasis was given to gain insight into the structure–reactivity correlation through detailed kinetic investigations of the synthesized complexes.

Experimental section

Materials and physical measurements

Cobalt(II) nitrate hexahydrate, *o*-aminophenol (OAPH), *o*-vanillin, and *N,N*-dimethyldipropylenetriamine were commercially available reagents and were used as received. Other chemicals and



Scheme 1 Schiff base HL.

solvents were purchased from commercial sources and used without further purification.

Caution! Azide salts of metal complexes especially with organic ligands are potentially explosive. Only a small amount of the material should be prepared and it should be handled with great care.

Elemental analyses (carbon, hydrogen and nitrogen) were performed using a Perkin-Elmer 240C elemental analyser. IR spectra were recorded as KBr pellets on a PerkinElmer Spectrum Two FTIR spectrophotometer in the range of 400 to 4000 cm^{-1} . Electronic absorption spectra were measured using an Agilent Carry-60 diode array UV-vis spectrophotometer at room temperature. Electrospray ionization mass spectrometry (ESI-MS positive) was performed using a Micromass Q-tof-Micro Quadrupole mass spectrophotometer. Cyclic voltammetric experiments were carried out at room temperature in methanol using tetrabutylammonium perchlorate as a supporting electrolyte on a CH Instrument electrochemical workstation model CHI630E with a three-electrode assembly comprising a platinum working electrode, a platinum wire auxiliary electrode and a Ag/AgCl reference electrode. The powder X-ray diffraction (PXRD) data were collected using a Bruker D8 Advance X-ray diffractometer using Cu-K α radiation ($\lambda = 1.5418 \text{ \AA}$) operating at 40 kV and 40 mA.

Synthesis of the Schiff-base ligand (HL). A tetradentate ligand (HL) was synthesized *via* the Schiff base condensation method. Briefly, 1.0 mmol of *N,N*-dimethyldipropylenetriamine (159 mg) and 1.0 mmol of *o*-vanillin (152 mg) were combined in 20 ml of methanol (or acetonitrile). The resulting mixture was allowed to reflux for *ca.* 1 h, and then cooled. The *in situ* prepared Schiff base ligand was directly used for the synthesis of the metal complexes adopting a general procedure as follows.

Synthesis of $[\text{Co}(\text{L})(\text{N}_3)_2] \cdot 0.5\text{CH}_3\text{CN}$ (1). $\text{Co}(\text{NO}_3)_2 \cdot 6\text{H}_2\text{O}$ (291 mg, 1.0 mmol) and Schiff base ligand HL (1.0 mmol) were combined in 40 ml acetonitrile, and to the mixture 2 ml of an aqueous solution of sodium azide (130 mg, 2.0 mmol) was added with stirring. The resulting mixture was heated to reflux for about 30 min during which time the colour of the solution changed to dark brown. The reaction mixture was then filtered and kept at ambient temperature for slow evaporation. Analytically pure dark-brown crystals suitable for X-ray diffraction were separated out from the solution within a week, which were collected by filtration and washed with methanol/ether and air dried. Yield: 392 mg (86%). Anal. calcd for $\text{C}_{34}\text{H}_{55}\text{Co}_2\text{N}_{19}\text{O}_4$: C 44.79%, H 6.08%, N 29.19%. Found: C 44.64%, H 6.05%, N 29.06%. FTIR (KBr, cm^{-1}): $\nu(\text{N}_3)$ 2033 vs; $\nu(\text{C}=\text{N})$ 1619 s.

Synthesis of complex $[\text{Co}(\text{L})(\text{NCS})_2] \cdot 0.5\text{H}_2\text{O}$ (2). Complex 2 was synthesized from an acetonitrile/water (20:1) mixture following a very similar procedure as described for 1, except that NH_4SCN was used instead of NaN_3 . Colour: dark brown, yield: 395 mg (83%). Anal. calcd for $\text{C}_{36}\text{H}_{54}\text{Co}_2\text{N}_{10}\text{O}_5\text{S}_4$: C 45.37%, H 5.71%, N 14.70%. Found: C 45.46%, H 5.65%, N 14.59%. FTIR (cm^{-1} , KBr): $\nu(\text{NCS})$ 2108 s, $\nu(\text{C}=\text{N})$ 1623 s.

Synthesis of complex $[\text{Co}(\text{HL})_2][\text{Co}(\text{NCS})_4] \cdot \text{NCS}$ (3). Complex 3 was synthesized from a methanol/water (20:1) mixture following the same methodology applied for the synthesis of 1, but NH_4SCN was used in place of NaN_3 . Colour: dark brown, yield:

358 mg (72%). Anal. calcd for $\text{C}_{37}\text{H}_{54}\text{Co}_2\text{N}_{11}\text{O}_4\text{S}_5$: C 44.66%, H 5.47%, N 15.48%. Found: C 44.51%, H 5.48%, N 14.39%. FTIR (cm^{-1} , KBr): $\nu(\text{NCS})$ 2067 s, $\nu(\text{C}=\text{N})$ 1615 s.

Synthesis of complex $[\text{Co}(\text{L})_2][\text{Co}(\text{NCO})_4]$ (4). Complex 4 was synthesized from an acetonitrile/water (20:1) mixture adopting an identical procedure as described for 1, except that NaNCO was used instead of NaN_3 . Colour: dark brown, yield: 295 mg (78%). Anal. calcd for $\text{C}_{68}\text{H}_{104}\text{Co}_3\text{N}_{16}\text{O}_{12}$: C 53.93%, H 6.92%, N 14.80%. Found: C 54.06%, H 6.95%, N 14.69%. FTIR (cm^{-1} , KBr): $\nu(\text{NCO})$ 2217 vs, $\nu(\text{C}=\text{N})$ 1626 s.

X-ray crystallography

Single crystal X-ray diffraction data for 1–4 were collected using a Bruker Kappa Apex-II CCD diffractometer, equipped with monochromated Mo-K α radiation ($\lambda = 0.71073 \text{ \AA}$). Data were collected in a wide range of φ and ω angles to increase the number of redundant reflections. The images obtained during the data collection for all complexes were processed with the software SAINT+, and the absorption effects were corrected by using the multi-scan method implemented in SADABS.⁴² The structures were solved using direct methods and refined by successive full-matrix least-squares cycles on F^2 using SHELXL-v.2013.⁴³ All the non-hydrogen atoms were successfully refined using anisotropic displacement parameters. Hydrogen atoms attached to carbon atoms were placed at geometrically idealized positions, and included in subsequent refinement cycles in riding-motion approximation with isotropic thermal displacement parameters fixed at 1.2 or 1.5 times that of the respective parent atoms. All other hydrogen atoms attached to the oxygen and nitrogen atoms were found in the Fourier difference maps, their distances and thermal displacement parameters were fixed in some cases and were allowed to refine with a riding model. Additional information related to crystallographic data collection and structure refinement details are summarized in Table 1.

Catalytic oxidation of *o*-aminophenol

Catalytic oxidation of *o*-aminophenol (OAPH) was carried out by the reaction of $1.0 \times 10^{-2} \text{ M}$ of OAPH with $2 \times 10^{-5} \text{ M}$ of the complexes in air-saturated methanol at room temperature. The reaction was followed spectrophotometrically by monitoring the progressive increase in the absorbance as a function of time at 434 nm ($\epsilon = 9095 \text{ M}^{-1} \text{ cm}^{-1}$),⁴⁴ which is characteristic of 2-aminophenoxazin-3-one in methanol. The catalytic efficiency of the complexes was examined by measuring time course spectral profiles using variable concentrations of the substrate with a fixed concentration ($2 \times 10^{-5} \text{ M}$) of the complexes under pseudo-first order conditions. All the kinetic measurements were carried out for the period of 10 min and the initial rate of the reaction was determined by linear regression from the slope of the absorbance *versus* time plot.

Results and discussion

Syntheses and general characterization

The condensation reaction of *N,N*-dimethyldipropylenetriamine with *o*-vanillin in a 1:1 molar ratio in methanol resulted

Table 1 Crystal data and structure refinement parameters of complexes 1 to 4

	1	2	3	4
Empirical formula	C ₃₄ H ₅₅ Co ₂ N ₁₉ O ₄	C ₁₈ H _{26.5} CoN ₅ O _{2.25} S ₂	C ₃₇ H ₅₄ Co ₂ N ₁₁ O ₄ S ₅	C ₆₈ H ₁₀₄ Co ₃ N ₁₆ O ₁₂
Formula weight (g mol ⁻¹)	911.83	471.99	995.07	1514.46
Temperature (K)	298(2)	150(2)	150(2)	298(2)
Crystal system	Monoclinic	Triclinic	Monoclinic	Tetragonal
Space group	C2/c	P $\bar{1}$	P2 ₁ /c	P4 ₂ /n
<i>a</i> (Å)	25.636(3)	7.9958(4)	18.977(3)	17.0179(4)
<i>b</i> (Å)	10.3538(4)	10.1437(5)	11.8646(17)	17.0179(4)
<i>c</i> (Å)	19.712(2)	13.4435(7)	21.938(3)	12.9851(4)
α (°)	90	85.118(2)	90	90
β (°)	126.446(16)	83.482(2)	108.078(4)	90
γ (°)	90	89.535(2)	90	90
Volume (Å ³)	4208.8(7)	1079.38(9)	4695.6(11)	3760.60(17)
<i>Z</i>	4	2	4	2
<i>D</i> _{calc} (mg m ⁻³)	1.439	1.452	1.408	1.337
μ (mm ⁻¹)	0.850	1.013	0.978	0.722
<i>F</i> (000)	1912	493	2076	1602
θ range (°)	1.98–28.29	2.56–29.20	2.12–26.51	1.69–25.40
Reflections collected	8285	37 750	121 708	55 064
Independent reflections (<i>R</i> _{int})	4591(0.0250)	5801(0.0270)	9653(0.0837)	3462(0.0832)
Observed reflections [<i>I</i> > 2 σ (<i>I</i>)]	3874	5130	6908	2261
Restraints/parameters	0/272	0/269	0/555	0/231
Goodness-of-fit on <i>F</i> ²	1.039	1.043	1.108	1.049
Final <i>R</i> indices [<i>I</i> > 2 σ (<i>I</i>)]	<i>R</i> ₁ = 0.0407 w <i>R</i> ₂ = 0.0972	<i>R</i> ₁ = 0.0253 w <i>R</i> ₂ = 0.0646	<i>R</i> ₁ = 0.0549 w <i>R</i> ₂ = 0.1409	<i>R</i> ₁ = 0.0380 w <i>R</i> ₂ = 0.0832
<i>R</i> indices (all data)	<i>R</i> ₁ = 0.0507 w <i>R</i> ₂ = 0.1030	<i>R</i> ₁ = 0.0315 w <i>R</i> ₂ = 0.0677	<i>R</i> ₁ = 0.0862 w <i>R</i> ₂ = 0.1767	<i>R</i> ₁ = 0.0738 w <i>R</i> ₂ = 0.0931
Largest diff. peak/hole (e Å ⁻³)	0.437/–0.350	0.402/–0.335	1.143/–1.063	0.170/–0.256

dark-orange Schiff base HL (Scheme 1). Treatment of this *in situ* generated Schiff base with cobalt(II) nitrate hexahydrate in the presence of pseudohalides (N₃⁻ for 1, NCS⁻ for 2 and 3, and NCO⁻ for 4) in a 1:1:2 molar ratio afforded [Co(L)(N₃)₂].0.5CH₃CN (1), [Co(L)(NCS)₂].0.5H₂O (2), [Co(HL)₂][Co(NCS)₄].NCS (3) and [Co(L)₂]₂[Co(NCO)₄] (4), in high yield. Although the stoichiometry of the reactants is found to be insensitive to the synthesis of these complexes, the distinguishing role of the solvents is observed for the synthesis of thiocyanate complexes. For instance, when the reaction is carried out in an acetonitrile/water mixture in the presence of NCS⁻, the only isolable product is 2, but when the same reaction was performed in a methanol/water mixture, we isolated only compound 3 in high yield. Isolation of both 2 and 3 from the same reactants suggests that both of them are present in equilibrium in solution, where the relative population in a particular solvent system governs the identity of the species that crystallizes from a given solution. To check whether they are interconvertible, we re-dissolved 2 and 3 in methanol and acetonitrile solvents, respectively, but upon standing at ambient temperature for a long period of time, no spectral change is noticed (Fig. S1, ESI[†]). These results indicate that both of them are thermodynamically stable products and formation of them is controlled by the solvents used for their synthesis. However, in all the complexes, the metal centre bonded to the Schiff base ligand is oxidized to Co(III) by aerial oxygen. All these complexes are air-stable and moisture insensitive, and are soluble in common organic solvents like methanol, acetonitrile and DMF. The purity of the bulk sample was verified by elemental analysis as well as by PXRD measurements (Fig. S2, ESI[†]).

The IR spectra of all complexes show strong and sharp bands in the range of 1615–1626 cm⁻¹, which are characteristic stretching vibrations of the azomethine bond of the Schiff base. In the spectrum of complex 1, a strong absorption band is observed at 2033 cm⁻¹, which is a characteristic stretching band of an azide ion.⁴⁵ Complexes 2 and 3 show two sharp absorption bands for thiocyanate ions, at 2108 and 2067 cm⁻¹, respectively.^{41,46} The relatively lower stretching vibration of the thiocyanate ion in 3 is associated with the greater π acceptor ability of the thiocyanate from a Co(II) ion compared to its π acceptor ability from a Co(III) centre in 2. A similar characteristic stretching band for a cyanate ion in 4 is observed at 2217 cm⁻¹.⁴⁵

Structural descriptions

Crystal structures of complexes 1–4 were determined by single-crystal X-ray diffraction; thermal ellipsoid plots of the structures of 1 and 2 with selected atom numbering schemes are depicted in Fig. 1, while Fig. 2 and 3 represent the molecular structures of 3 and 4, respectively. Important bond distances for the metal coordination sphere for all structures are given in Table 2. Neutral complexes 1 and 2 crystallize on general positions – 1 incorporates a disordered acetonitrile molecule with half occupancy on a 2-fold axis, while 2 crystallizes with a water molecule of half occupancy on a general position. The structures of both 1 and 2 are eventually similar in that the Co(III) centre is hexacoordinated with distorted octahedral geometry as reflected from the significant deviation of the cisoid (83.83(9)–94.46(5)°) and transoid (173.65(4)–176.62(5)°) angles from the ideal values. The deprotonated Schiff base ligand (L) is bonded to the metal centre with phenolate-O and three nitrogen atoms (one each of imine, secondary amine and

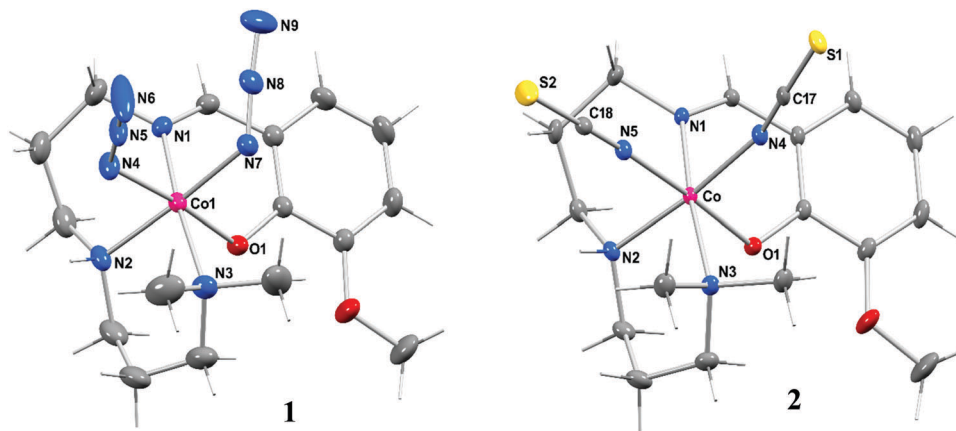


Fig. 1 Crystal structures of **1** and **2** showing selected atom numbering schemes. Thermal ellipsoids are drawn at 30% probability.

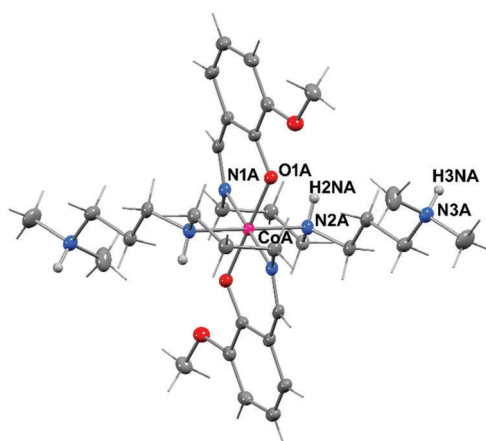


Fig. 2 Crystal structure of one of the crystallographically independent complex cations of **3** with the selected atom labelling scheme. Ellipsoids are drawn at 30% probability.

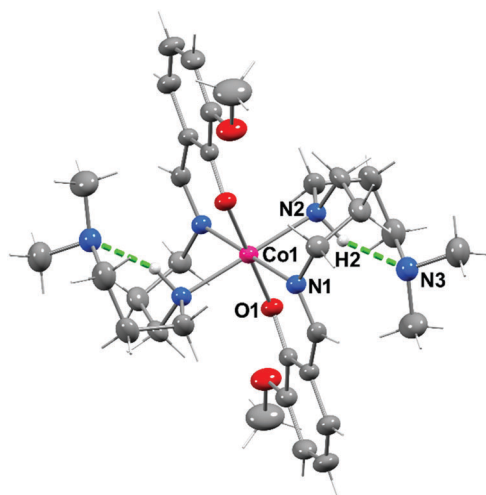


Fig. 3 Crystal structure of the complex cation of **4** with the selected atom numbering scheme. Ellipsoids are drawn at 30% probability.

tertiary amine nitrogen atoms) and the two remaining positions are occupied by two nitrogen atoms from two terminal azide

Table 2 Selected bond distances (Å) for complexes **1–4**

Bond	1	2	3	4
Co(III)–N(imine)	1.9302(18)	1.9298(11)	1.943(3)	1.9336(18)
Co(III)–N(secondary amine)	2.0115(18)	1.9816(11)	1.941(3)	2.0117(19)
Co(III)–N(tertiary amine)	2.112(2)	2.1038(11)	2.043(3)	2.043(3)
Co(III)–O(phenolate)	1.8862(14)	1.8608(9)	1.886(2)	1.8884(15)
Co(III)–N(pseudohalide)	1.940(19)	1.9187(11)	1.896(2)	—
Co(II)–N(pseudohalide)	—	—	1.946(4)	1.948(3)
			1.947(4)	—
			1.962(4)	—
			1.968(4)	—

(in **1**) and thiocyanate (in **2**) ions. Again, in both cases, three nitrogen atoms from the triamine part of the Schiff base occupy one meridional position, while two nitrogen atoms of pseudohalides along with the phenolate-O atom of the Schiff base occupy other meridional position. The Co–N distances of the pseudohalides and the Co–O distances of the phenolate group of the tetradentate L ligand in **1** and **2** vary in the range of 1.8608(9)–1.8862(16) and 1.9187(11)–1.952(2) Å, respectively, which are comparable to the bond distances observed in analogues low-spin octahedral Co(III) complexes.^{47–49} In both complexes, the Co–N bond distances reveal that secondary amine bonds are somewhat longer than the imine moieties in both complexes (see Table 2), which is consistent with the state of hybridization of respective nitrogen atoms. But the significantly longer bond distance of the tertiary amine over the secondary amine groups found in these structures probably arises from the increased steric congestion around the metal centre due to the presence of two methyl substitutions at the tertiary nitrogen, thereby leading to the weaker binding ability of the tertiary amine in these complexes.⁴¹ Furthermore, the N–N distances of azide ions [1.181(3)–1.192(3) Å] between the central nitrogen and the nitrogen bonded to the metal centre are somewhat longer than the terminal N–N bonds [1.142(3)–1.144(3) Å], which is typical for coordination through the anionic terminal of an azide ion.^{47,49} Again, as found in similar

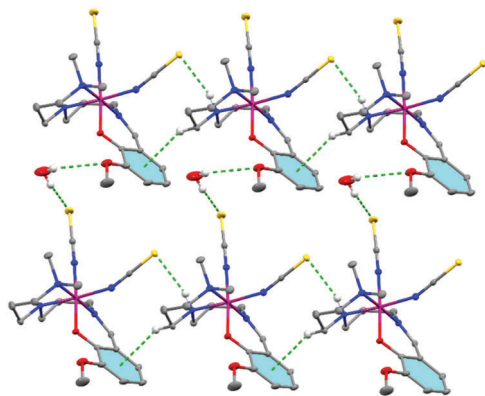


Fig. 4 A part of the packing showing hydrogen bonding and C–H... π interactions in **2**.

complexes, the thiocyanate is coordinated through the nitrogen end in **2**.^{41,46} The crystal packing of **1** is stabilized by hydrogen bonding interactions (Table S1, ESI[†]) involving the secondary amine and a solvent acetonitrile molecule as shown in Fig. S3 (ESI[†]). The stability in the solid state is further reinforced by C–H... π interactions between the adjacent molecules (Table S2, ESI[†]). The solid state structure of **2** is stabilized by multiple hydrogen bonding interactions (Table S1, ESI[†]) in which a crystallized water molecule simultaneously interacts with the sulphur atom of a thiocyanate ion and the methoxy oxygen atom from two different complex molecules (Fig. 4). Another thiocyanate ion is also connected with a secondary amine group from a neighbouring molecule through hydrogen bonding. C–H... π interaction (Table S2, ESI[†]) involving two adjacent complexes further stabilizes the overall supramolecular structure of **2** in the *ab* plane.

Unlike **1** and **2**, both **3** and **4** are ionic compounds. Complex **3** crystallizes in the monoclinic $P2_1/c$ space group such that the asymmetric unit includes two crystallographically independent complex cations of composition $[\text{Co}(\text{HL})_2]^{3+}$ on inversion centres and two different anions $\text{Co}(\text{NCS})_4^{2-}$ and NCS^- on general positions. Complex **4** on the other hand crystallizes in the tetragonal space group $P4_2/n$ where the complex cation, $[\text{Co}(\text{L})_2]^+$, sits on an inversion centre, while the complex anion $\text{Co}(\text{NCO})_4^{2-}$ resides on a 4-fold axis. Although the structures of **3** and **4** are apparently similar, they are significantly different from each other from the charge neutralization point of view. Crystallization of both anions $\text{Co}(\text{NCS})_4^{2-}$ and NCS^- on general positions requires the protonation of the tertiary amine-N of the Schiff base ligands for balancing the charge in **3**, while it is not protonated in complex **4**. Although in both cases, the potentially tetradentate Schiff base ligand binds the metal centre in a tridentate fashion, the zwitterionic form of the Schiff base is coordinated to the metal centre in **3**, while it is monoanionic in **4** but bonded with the metal centre using three donor sites leaving the tertiary amine group free from coordination. The geometry of both $\text{Co}(\text{NCS})_4^{2-}$ and $\text{Co}(\text{NCO})_4^{2-}$ is tetrahedral in which the pseudohalides are coordinated to cobalt(II) ions through the nitrogen atoms.^{50–52} The N–Co–N bond angles varying in the range of 104.10(17)–115.12(17) and

108.44(8)–111.55(17)[°] for **3** and **4**, respectively, are in agreement with the tetrahedral geometry. In the complex cations, the geometry of a cobalt(III) centre is found to be pseudo-octahedral and it is coordinated by two Schiff base ligands, each of which occupies a facial position and binds the metal centre through the phenolate-O, imine-N and secondary amine-N. The Co–N distances of the imine and secondary amine and the Co–O distances of the phenolate group of the Schiff base ligand in **3** and **4** vary in the range of 1.9338(18)–1.943(3), 2.0116(19)–2.044(3) and 1.886(2)–1.896(2) Å, respectively, which are comparable to bond distances observed in **1** and **2** and also in analogous low-spin octahedral Co(III) complexes with similar coordination environments.^{47–49} As observed in **1** and **2**, the imine bonds are somewhat shorter than the secondary amine nitrogen in **3** and **4**, which is the consequence of their respective state of hybridization. The solid state structures of **3** and **4** are stabilized by noncovalent interactions like hydrogen bonding and C–H... π interactions (Table S2, ESI[†]). The most striking difference in the noncovalent interactions in these compounds mainly arises from the hydrogen bonding interactions. Whereas the tertiary amine nitrogen in the Schiff base ligand is not protonated in **4**, thereby it is involved in intramolecular hydrogen bonding with the secondary amine from the same ligand (Fig. S4, ESI[†]). The tertiary amine nitrogen in **3** is on the other hand protonated, which brings different hydrogen bonding patterns in the system (Table S1, ESI[†]). Careful inspection of the solid state packing of **3** shows that the protonated tertiary amine nitrogen is engaged in strong hydrogen bonding with the nitrogen atom of a thiocyanate counterion that is simultaneously involved in hydrogen bonding with the protonated tertiary amine of the adjacent complex cation through a sulphur atom, leading to a 1D chain propagating along the *a* axis (Table S1, ESI[†]). This supramolecular chain structure is further supported by the noncovalent interactions offered by $\text{Co}(\text{NCS})_4^{2-}$ which is involved in N–H...S hydrogen bonding and N–H... π interactions with two different complex cations as displayed in Fig. S5 (ESI[†]). The C–H... π interaction involving NCO^- ions in $\text{Co}(\text{NCO})_4^{2-}$ and the azomethine C–H of the complex cation further contribute to the solid state packing in **4** (Fig. S4, ESI[†]).

As a whole, the structural analyses reveal the versatile binding ability of the present Schiff base ligand in these systems. It can either coordinate the metal centre in a tetradentate fashion through the monoanionic deprotonated form using all four donor sites (in **1** and **2**) or in a tridentate fashion using the zwitterionic form of the Schiff base ligand leaving the quaternary amine nitrogen free from coordination (in **3**). Moreover, the monoanionic deprotonated ligand can also bind the metal centre in a tridentate fashion where the pendent tertiary amine nitrogen is involved in intramolecular hydrogen bonding in **4**. Furthermore, in our recent report with a Ni(II) system, it was observed that the triamine part of the Schiff base ligand binds the metal centre facially,⁴¹ while it is meridionally coordinated with the metal centre in the present systems (**1** and **2**). Therefore, all these above versatilities associated with this triamine suggest that the ligands derived from this

triamine could be useful in developing coordination chemistry with diverse structures.

Electrochemical studies

The redox potential of the active site of a metalloenzyme plays an important role in the catalytic oxidation of biochemical compounds in natural systems. Therefore, an electrochemical study especially under identical conditions to the catalytic study of the synthetic analogues could provide useful information about the catalytic ability of these compounds. In this context, the electrochemical behaviours of all complexes have been examined in methanol in the presence of 0.1 M tetrabutylammonium perchlorate as a supporting electrolyte at ambient temperature. Representative cyclic voltammograms of **2** and **3** are depicted in Fig. 5 and 6, respectively. Scanning in the cathodic direction, an irreversible reduction response was found at -0.77 and -0.71 V for **1** and **2**, respectively, which is a consequence of the reduction of Co(III) to Co(II) at the electrode surface. This irreversible electrode process is due to a significant modification of the reduced species at the electrode surface in terms of loss of azide or thiocyanate ions from the metal centres. Unlike **1** and **2**, the cyclic voltammograms of **3** and **4** consist of an irreversible oxidative response (0.99 V for **3** and 1.01 V for **4**) in addition to the reductive response (-0.92 V for **3** and -0.94 V for **4**). The reduction process is responsible for the reduction of Co(III) to Co(II) of the complex cations at the electrode surface, whereas the oxidative response is due to the oxidation of Co(II) to Co(III) of the complex anions of general formula $[\text{CoX}_4]^{2-}$ ($\text{X} = \text{SCN}$ for **3** and NCO for **4**). Electrochemical irreversibility again suggests the instability of the oxidized species at the electrode surface.

Phenoxazinone synthase mimicking activity

Phenoxazinone synthase like activity of the complexes was examined by monitoring the catalytic oxidation of commonly

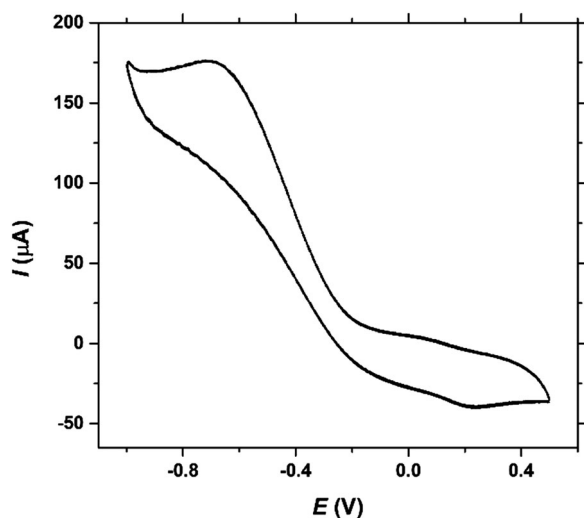


Fig. 5 Cyclic voltammograms of **2** in methanol using a platinum working electrode in the presence of tetrabutylammonium perchlorate as a supporting electrolyte at room temperature with a scan rate of 100 mV s^{-1} .

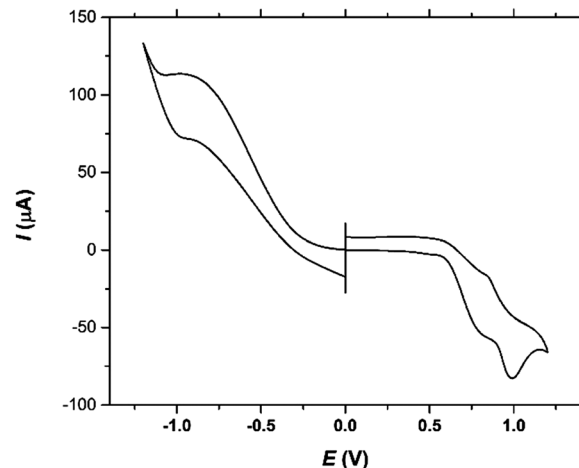


Fig. 6 Cyclic voltammograms of **3** in methanol using a platinum working electrode in the presence of tetrabutylammonium perchlorate as a supporting electrolyte at room temperature with a scan rate of 100 mV s^{-1} .

used substrate *o*-aminophenol (OAPH) UV-vis spectrophotometrically in dioxygen-saturated methanol at room temperature.³⁶ At first, it is important to confirm the ability of the synthesized complexes to oxidize OAPH. Accordingly, 2.0×10^{-5} M methanolic solutions of these complexes were combined with a 0.01 M solution of OAPH under aerobic conditions. The progress of the reaction was monitored by UV-vis spectrophotometry, and time-dependent spectral profiles, scanning with 5 min time intervals, after the addition of OAPH are presented in Fig. 7–9 for **1**, **2** and **4** respectively, and in Fig. S6 (ESI[†]) for **3**. The spectral scans reveal the cumulative growth of the peak intensity at *ca.* 434 nm, characteristic of the phenoxazinone chromophore, suggesting the catalytic oxidation of OAPH to 2-aminophenoxazin-3-one under aerobic conditions. These spectral behaviours unambiguously demonstrate that all complexes are active catalysts for the aerial

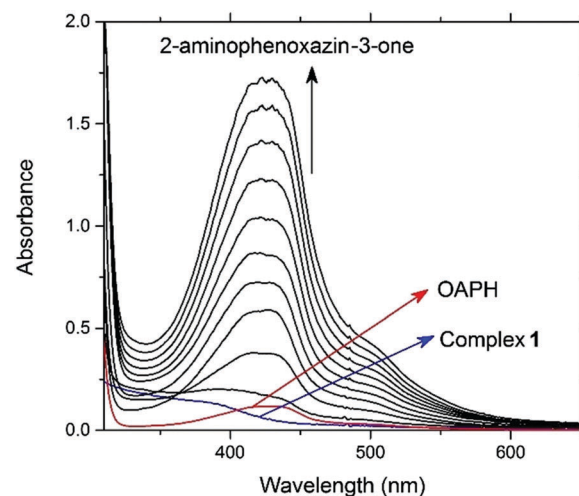


Fig. 7 Time dependent UV-vis spectral changes for the oxidation of *o*-aminophenol (1.0×10^{-2} M) catalysed by **1** (2×10^{-5} M) in dioxygen-saturated methanol. The spectra were recorded at 5 min intervals under aerobic conditions at room temperature.

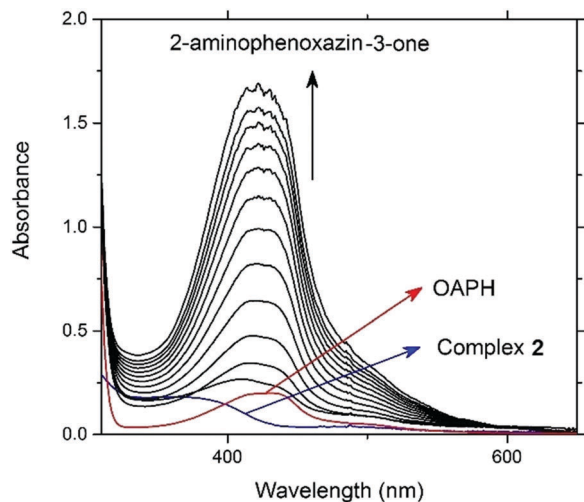


Fig. 8 Time dependent spectral scan showing growth of 2-aminophenoxazin-3-one at 434 nm upon addition of 1.0×10^{-2} M OAPH to a solution containing **2** (2×10^{-5} M) in dioxygen-saturated methanol. The spectra were recorded at 5 min intervals under aerobic conditions at room temperature.

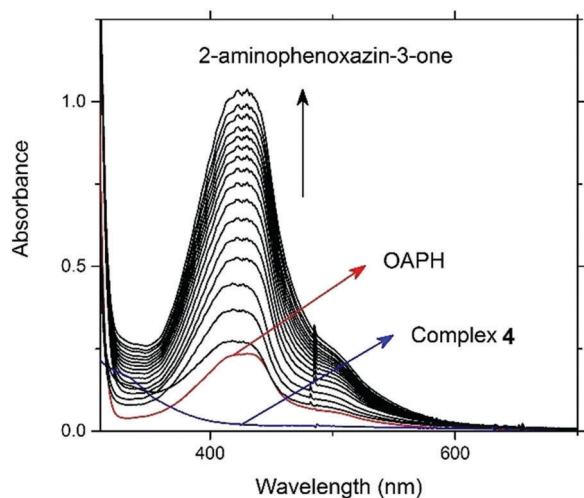


Fig. 9 The time resolved spectral profile showing oxidation of *o*-aminophenol (1.0×10^{-2} M) catalysed by **4** (2×10^{-5} M) in dioxygen-saturated methanol. The spectra were recorded at 5 min intervals under aerobic conditions at room temperature.

oxidation of OAPH to the corresponding phenoxazinone chromophore. Spectral profiles further suggest that although complexes **1**, **2** and **4** are efficient catalysts for OAPH oxidation, the reactivity of complex **3** is significantly low. Detailed reaction kinetics was further performed to understand the extent of the catalytic efficiency. For this purpose, a 2.0×10^{-5} M solution of the complexes was treated with at least 10-fold excess of the substrate to follow the pseudo-first-order conditions, and the time scan at the maximum band (434 nm) of 2-aminophenoxazin-3-one was carried out for a period of 10 min, and the initial rate was determined by linear regression from the slope of the absorbance *versus* time plot, considering the extinction coefficient of 2-aminophenoxazin-3-one as $9095 \text{ M}^{-1} \text{ cm}^{-1}$ in methanol.⁴⁴ The initial rate *versus* substrate

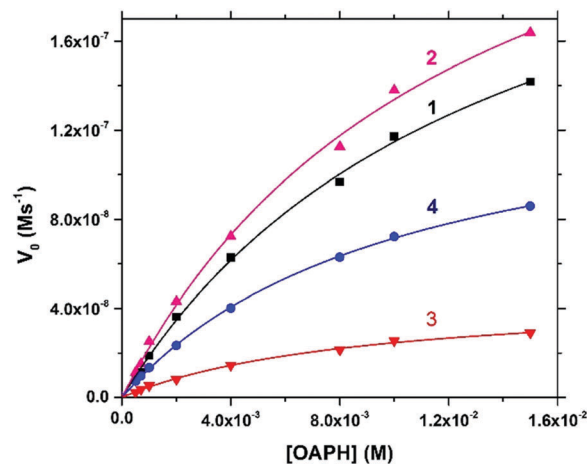


Fig. 10 Initial rate *versus* substrate concentration plot for the oxidation of OAPH in dioxygen-saturated methanol catalysed by **1–4** at room temperature. Symbols and solid lines represent the experimental and simulated profiles, respectively.

concentration plots show rate saturation kinetics as depicted in Fig. 10. These observations unambiguously conclude that an intermediate complex-substrate adduct is formed in a pre-equilibrium stage followed by the irreversible redox transformation of the intermediate in the rate determining step of the catalytic cycle. The Michaelis-Menten model as well as its linear double reciprocal Lineweaver-Burk plot can be applied to analyse the values of the parameters V_{max} , K_{M} and K_{cat} . The observed and simulated nonlinear initial rate *versus* substrate concentration plot and the Lineweaver-Burk plot for all complexes are shown in Fig. 10 and Fig. S7 (ESI[†]), respectively. Analysis of the experimental data yielded Michaelis binding constant (K_{M}) values of 1.35×10^{-2} , 1.24×10^{-2} , 8.87×10^{-3} and 1.02×10^{-2} M for **1–4**, respectively, and V_{max} values of 3.00×10^{-7} , 2.70×10^{-7} , 4.65×10^{-8} and $1.45 \times 10^{-7} \text{ M s}^{-1}$ for **1–4**, respectively. The turnover number (k_{cat}) value is obtained by dividing V_{max} by the concentration of the complex used (2.0×10^{-5} M), and is calculated to be 54.0, 48.6, 26.1 and 8.37 h^{-1} for **1–4**, respectively.

Plausible mechanism and comparative catalytic activity

From the detailed kinetic analysis, it is clear that complexes **1** and **2** are efficient catalysts for the aerobic oxidation of *o*-aminophenol, while compounds **3** and **4** are relatively less reactive. These pseudohalide bound complexes favour the substrate binding by the loss of two coordinated pseudohalides, which is the main reason behind the excellent reactivity of both **1** and **2**. Slightly greater reactivity of the azide complex compared to the thiocyanate analogue is probably due to the better lability of azide over a thiocyanate ion. The mass spectral study could provide valuable information from which the most possible mechanism of the catalytic cycle can be framed. Therefore, the electrospray ionization mass spectrum (ESI-MS positive) of a representative compound **2** in the presence of 50 equivalents of *o*-aminophenol in acetonitrile was recorded after 15 min of mixing, and the spectrum is depicted in Fig. 11. Interestingly, the mass spectrum is clean enough as it only

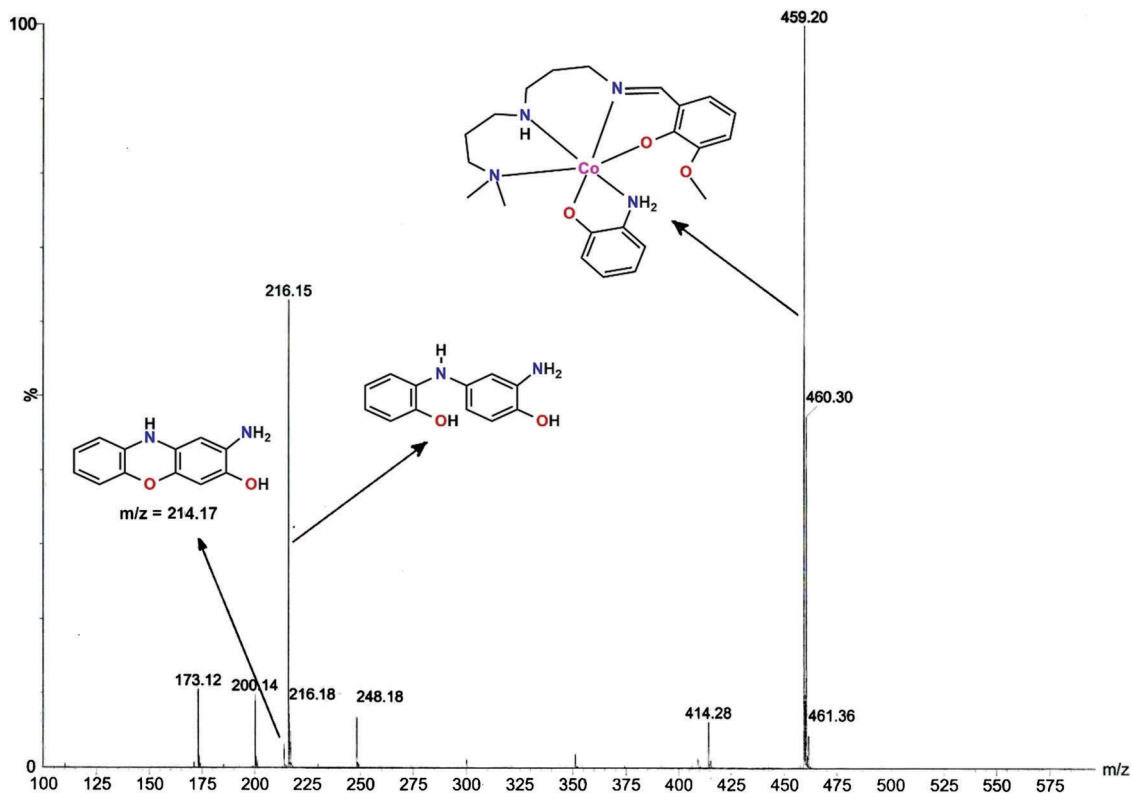


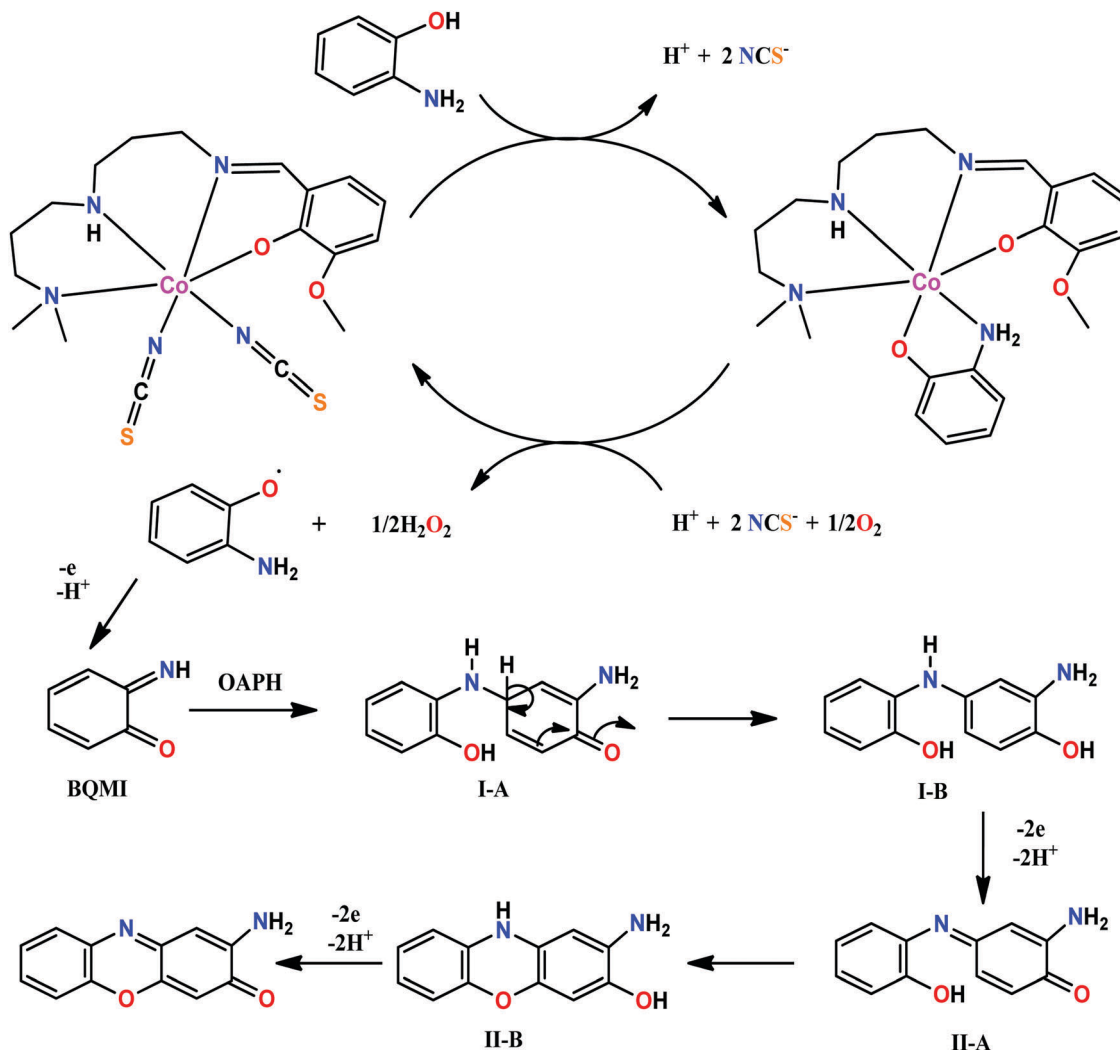
Fig. 11 Electrospray ionization mass spectrum (ESI-MS positive) of a 1:50 mixture of complex **2** and *o*-aminophenol in acetonitrile recorded after 15 min of mixing.

comprises a small numbers of peaks and all of them are well assignable. Remarkably, the base peak at $m/z = 459.20$ is a 1:1 complex–substrate aggregate of a monocationic species of composition $[\text{Co}^{\text{III}}(\text{L})(\text{OAP})]^+$ (calculated $m/z = 459.18$), establishing the formation of a stable complex–substrate adduct. The relative population of the original complex cation generated from the loss of a coordinated thiocyanate ion, $[\text{Co}^{\text{III}}(\text{L})(\text{NCS})]^+$ (calculated $m/z = 409.11$; found at $m/z = 409.23$), is about only 1% compared to the most abundant peak of the complex–substrate aggregate, and thereby establishes the ease of formation of the complex–substrate aggregate, exploiting the stronger chelating ability of an *o*-aminophenolate ion. Two other cobalt containing species are located at $m/z = 351.29$ and 414.28 and these peaks are assigned to $[\text{Co}^{\text{II}}(\text{L})]^+$ and $[\text{NaCo}^{\text{II}}(\text{L}-\text{H})]^+$, respectively. Furthermore, a lithium adduct of ligand HL is observed at $m/z = 300.14$. The peaks at $m/z = 173.12$ and 200.14 are assignable to the sodium adduct of the substrate along with solvent acetonitrile, $[\text{Na}(\text{OAPH})(\text{MeCN})]^+$, and an aggregate of the protonated OAPH and five water molecules, respectively. The peak at $m/z = 248.18$ is related to a peak of the molecular ion of the product 2-aminophenoxazin-3-one combined with two water molecules. The second highest abundant peak at $m/z = 216.15$ along with a minor peak at $m/z = 214.17$ is the most remarkable finding of this mass spectral study as these are related to the molecular ion peaks of two important reactive intermediates generated during the course of oxidative coupling of *o*-aminophenol as drawn in Scheme 2. This kind of information was not readily

available from most of the preceding mass spectral studies of the reported synthetic models of phenoxazinone synthase, and in some cases it is wrongly assigned.⁵³ Therefore, the present finding with proper assignment could provide significant information in the mechanistic study of phenoxazinone synthase.

Now at this stage, both the mass spectral study and rate saturation kinetics unambiguously conclude that the catalytic cycle for the aerobic oxidation of *o*-aminophenol catalysed by **1** and **2** starts with the formation of a complex–substrate aggregate by the replacement of the coordinated pseudohalides by *o*-aminophenol. This complex–substrate intermediate at the rate determining step generates an OAP radical through inner sphere electron transfer from *o*-aminophenolate to the metal centre. The OAP radical thereafter may generate *o*-benzoquinone monoamine (BQMI) in many ways including the disproportionation of the OAP radical itself. This BQMI is then reacted with another OAPH to generate a reactive intermediate **I-B** as suggested by the mass spectral study, which thereafter undergoes two electron oxidation with molecular oxygen probably by the assistance of the complexes to produce another reactive intermediate **II-B**, again supported by the mass spectral study. Finally, 2-aminophenoxazin-3-one is produced from the oxidative dehydrogenation of intermediate **II-B** by the complexes as a catalyst as shown in Scheme 2.

The lower reactivity of compounds **3** and **4** compared to **1** and **2** is quite reasonable as the labile sites for substrate



Scheme 2 Plausible mechanistic pathway for the aerobic oxidation of *o*-aminophenol catalysed by **1** and **2**.

binding are not available for these systems, leading to catalytic activity through the outer sphere electron transfer pathway. These types of complexes are often found to be inactive,⁵⁴ but in the present case, especially compound **4** is found to be significantly catalytically active towards phenoxazinone synthase. In our previous study, we observed that the positive charge at the ligand backbone brings significantly enhanced catalytic activity in which the positive charge of the pyridinium moiety at the ligand backbone may attract the substrate OAPH towards the formation of the complex–substrate adduct, leading to the enhanced catalytic activity in that system.⁵⁵ In the present case, the pendent tertiary amine group is protonated in **3**, while it is not protonated in **4**. As seen earlier, if simply the positive charge at the second coordination sphere is the crucial factor, then one can expect that compound **3** would show better catalytic activity than complex **4**. But in reality, we have observed that compound **4** exhibits significantly higher activity than complex **3**. In order to explore how the protonation/deprotonation at the second coordination sphere alter the catalytic activity in these systems, a series of 2×10^{-5} M solutions of **3** in methanol was

prepared by adding a varying amount of a tetrabutylammonium hydroxide base, and then these complex solutions were mixed

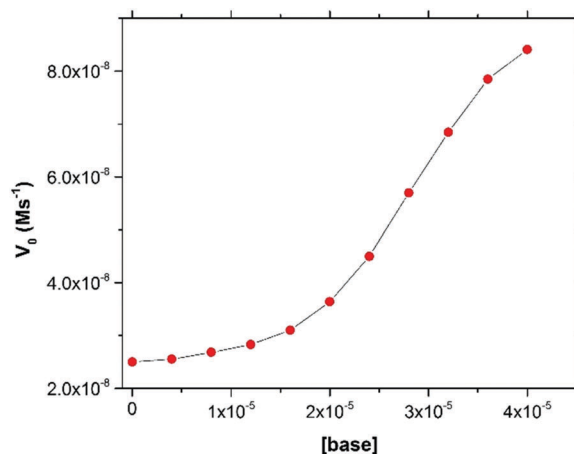
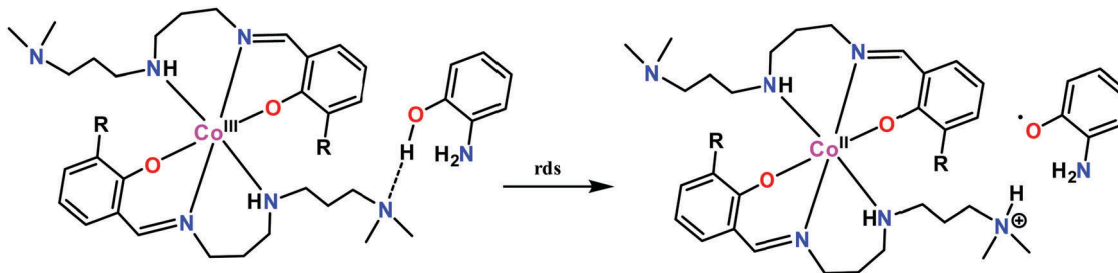


Fig. 12 Plot of initial rate vs. concentration of an added base for the aerobic oxidation of *o*-aminophenol (0.01 M) catalyzed by complex **3** (2×10^{-5} M).



Scheme 3 Stabilization of the intermediate through hydrogen bonding and facilitating oxidation of *o*-aminophenol by proton abstraction.

with 0.01 M substrate and the time course of the reaction is monitored UV-vis spectrophotometrically. As shown in Fig. 12, the catalytic activity of the complex increases with an increase in the added base and finally the rate of the reaction of **3** becomes comparable to the rate of **4**. This observation establishes that the deprotonation of quaternary amine at the second coordination sphere brings the higher activity in the system. This result suggests that not the positive charge but the hydrogen bond acceptor ability of the second coordination sphere is the foremost criterion for the substrate recognition and stability of the intermediate for enhanced catalytic activity (see Scheme 3). Furthermore, tertiary amine nitrogen abstracts a proton from *o*-aminophenol and facilitates the oxidation of OAPH, leading to the formation of the OAP radical at the rate determining step. When the tertiary amine is protonated, such proton abstraction from the substrate is not possible and thus oxidation of *o*-aminophenol is not favored. Therefore, the present study discloses that if the strong hydrogen bond acceptor center is present at the secondary coordination sphere, it can not only recognize the substrate and stabilize the complex substrate intermediate through hydrogen bonding, but also abstract a proton from the substrate and thereby facilitate oxidation of a substrate like *o*-aminophenol. This result clearly justifies the fact that the incredible reactivity of metalloenzymes in biological systems is not only due to the presence of available labile position(s) for substrate binding but also due to the crucial role of the protein chain that helps in substrate recognition and stabilisation of the intermediate through various noncovalent forces.

Conclusions

In summary, we have synthesized a new tetradentate N_3O donor ligand by the Schiff base condensation of *N,N*-dimethyldi-propylenetriamine and *o*-vanillin. Using this Schiff base four new cobalt complexes have been prepared in the presence of pseudohalides in high yields, and the influence of the solvents on their syntheses has been noticed. X-ray crystal structure analyses reveal that the Schiff base can bind the metal centre either in a tetradentate fashion through the monoanionic deprotonated form using all four donor sites (in **1** and **2**) or in a tridentate fashion using the zwitterionic form of the Schiff base ligand with a pendent quaternary amine nitrogen, which establishes intramolecular hydrogen bonding with the secondary amine group from the same ligand (in **3**). The monoanionic deprotonated ligand can also coordinate the metal centre in a

tridentate fashion (in **4**) where the pendent tertiary amine nitrogen is utilized in the formation of intramolecular hydrogen bonding. It is worth noting that, in our recent report with a Ni(II) system, the triamine part of the Schiff base ligand binds the metal centre facially, while it is meridionally coordinated with the metal centre in the present systems (**1** and **2**). Therefore, all these versatilities associated with this triamine make it a promising synthon for the development of coordination chemistry with diverse structures. All complexes exhibit strong phenoxazinone synthase activity, and as expected the availability of binding sites at the first coordination sphere for the substrate, *o*-aminophenol, is responsible for significantly higher catalytic activity in **1** and **2**. The presence of a hydrogen bond acceptor site at the second coordination sphere in **4** not only stabilizes the complex-substrate outer sphere association complex but also abstracts a proton from *o*-aminophenol, thereby facilitating oxidation of the substrate. From the ESI mass spectral data of **2** in the presence of 50 equivalents of *o*-aminophenol, several important intermediates have been assigned, which provides significant information regarding the mechanistic pathway of the functioning phenoxazinone synthase activity of the synthetic models. This result therefore directs the development of coordination compounds having both labile or vacant positions at the first coordination sphere for substrate binding and a hydrogen bond acceptor cum proton abstraction centre at the second coordination sphere for better biomimetic catalysts that have a higher degree of structural resemblance with the metalloenzymes.

Acknowledgements

A. P. would like to thank the University Grant Commission, New Delhi, for financial support. The authors thank Indian Institute of Chemical Biology, Kolkata for providing the Mass spectral facility.

References

- 1 S. I. Murahashi and Y. Imada, in *Transition Metals for Organic Synthesis*, ed. M. Beller and C. Bolm, Wiley-VCH, Weinheim, Germany, 2nd edn, 2004, vol. 2, p. 497.
- 2 J. Gómez, G. García-Herbosa, J. V. Cuevas, A. Arnáiz, A. Carbayo, A. Muñoz, L. Falvello and P. E. Fanwick, *Inorg. Chem.*, 2006, **45**, 2483.

- 3 *Dioxygenases in Catalysis by Metal Complexes, Oxygenases and Model Systems*, ed. T. Funabiki, Kluwer Academic, Dordrecht, 1997, p. 19.
- 4 J. P. Klinman, *JBIC, J. Biol. Inorg. Chem.*, 2011, **16**, 1.
- 5 *Dioxygen Reactions in Bioinorganic Chemistry*, ed. I. Bertini, H. B. Gray, S. J. Lippard and J. S. Valentine, University Science Books, Sausalito, 1994, p. 253.
- 6 The chemistry and activation of dioxygen species (O_2 , O_2^- and H_2O_2) in biology, in *Oxygen Complexes and Oxygen Activation by Transition Metals*, ed. A. E. Martell and D. T. Sawyer, Plenum, New York, 1988, p. 131.
- 7 E. I. Solomon, T. C. Brunold, M. I. Davis, J. N. Kemsley, S. K. Lee, N. Lehnert, F. Neese, A. J. Skulan, Y. S. Yang and J. Zhou, *Chem. Rev.*, 2000, **100**, 235.
- 8 E. I. Solomon, R. Sarangi, J. S. Woertink, A. J. Augustine, J. Yoon and S. Ghosh, *Acc. Chem. Res.*, 2007, **40**, 581.
- 9 E. G. Kovaleva and J. D. Lipscomb, *Nat. Chem. Biol.*, 2008, **4**, 186.
- 10 S. S. Stahl, *Science*, 2005, **309**, 1824.
- 11 *Advances in Catalytic Activation of Dioxygen by Metal Complexes*, ed. L. I. Simándi, Springer, New York, 2003.
- 12 *Biomimetic Oxidations Catalyzed by Transition Metal Complexes*, ed. B. Meunier, Imperial College, London, 2000.
- 13 P. Chaudhuri and K. Wieghardt, *Prog. Inorg. Chem.*, 2001, **50**, 151.
- 14 R. H. Holm and E. I. Solomon, *Chem. Rev.*, 2004, **104**, 347.
- 15 C. Mukherjee, T. Weyhermüller, E. Bothe, E. Rentschler and P. Chaudhuri, *Inorg. Chem.*, 2007, **46**, 9895.
- 16 P. Chaudhuri, K. Wieghardt, T. Weyhermüller, T. K. Paine, S. Mukherjee and C. Mukherjee, *Biol. Chem.*, 2005, **386**, 1023.
- 17 U. Jhan, *Top. Curr. Chem.*, 2004, **320**, 323.
- 18 S. E. Allen, R. R. Walvoord, R. Padilla-Salinas and M. C. Kozlowski, *Chem. Rev.*, 2013, **113**, 6234.
- 19 T. K. Paine and L. Que, Jr., *Struct. Bonding*, 2014, **160**, 39.
- 20 L. A. Joyce, S. H. Shabbir and E. V. Anslyn, *Chem. Soc. Rev.*, 2010, **39**, 3621.
- 21 J. Meeuwissen and J. N. H. Reek, *Nat. Chem.*, 2010, **2**, 615.
- 22 J. V. Bannister, W. H. Bannister and G. Rotilio, *CRC Crit. Rev. Biochem.*, 1987, **22**, 111.
- 23 M. Shyamal, T. K. Mandal, A. Panja and A. Saha, *RSC Adv.*, 2014, **4**, 53520.
- 24 N. C. Jana, P. Brandão and A. Panja, *J. Inorg. Biochem.*, 2016, **159**, 96.
- 25 A. Panja, N. C. Jana, A. Bauzá, S. Adak, T. M. Mwanja, D. M. Eichhorn and A. Frontera, *ChemistrySelect*, 2017, **2**, 2094.
- 26 A. Panja and P. Guionneau, *Dalton Trans.*, 2013, **42**, 5068.
- 27 A. Panja, *RSC Adv.*, 2014, **4**, 37085.
- 28 C. E. Barry, P. G. Nayar and T. P. Begley, *J. Am. Chem. Soc.*, 1988, **110**, 3333.
- 29 E. Frei, *Cancer Chemother. Rep., Part 1*, 1974, **58**, 49.
- 30 U. Hollstein, *Chem. Rev.*, 1974, **74**, 625.
- 31 L. I. Simándi, T. M. Simándi, Z. May and G. Besenyi, *Coord. Chem. Rev.*, 2003, **245**, 85.
- 32 M. Hassanein, M. Abdo, S. Gerges and S. El-Khalafy, *J. Mol. Catal. A: Chem.*, 2008, **287**, 53.
- 33 T. M. Simándi, L. I. Simándi, M. Győr, A. Rockenbauer and Á. Gömör, *Dalton Trans.*, 2004, 1056.
- 34 T. Horváth, J. Kaizer and G. Speier, *J. Mol. Catal. A: Chem.*, 2004, **215**, 9.
- 35 J. Kaizer, G. Baráth, R. Csonka, G. Speier, L. Korecz, A. Rockenbauer and L. Párkányi, *J. Inorg. Biochem.*, 2008, **102**, 773.
- 36 S. K. Dey and A. Mukherjee, *Coord. Chem. Rev.*, 2016, **310**, 80.
- 37 S. Sagar, S. Sengupta, A. J. Mota, S. K. Chattopadhyay, A. E. Ferao, E. Riviere, W. Lewis and S. Naskar, *Dalton Trans.*, 2017, **46**, 1249.
- 38 A. Jana, N. Aliaga-Alcalde, E. Ruiz and S. Mohanta, *Inorg. Chem.*, 2013, **52**, 7732.
- 39 P. Mahapatra, S. Ghosh, S. Giri, V. Rane, R. Kadam, M. G. B. Drew and A. Ghosh, *Inorg. Chem.*, 2017, **56**, 5105.
- 40 A. Company, L. Gomez, R. Mas-Balleste, I. V. Korendovych, X. Ribas, A. Poater, T. Parella, X. Fontrodona, J. Benet-Buchholz, M. Sola, L. Que Jr, E. V. Rybak-Akimova and M. Costas, *Inorg. Chem.*, 2007, **46**, 4997.
- 41 A. Panja, N. C. Jana, S. Adak, P. Brandão, L. Dlhán, J. Titiš and R. Boča, *New J. Chem.*, 2017, **41**, 3143.
- 42 G. M. Sheldrick, *SADABS*, University of Göttingen, Germany, 1996.
- 43 G. M. Sheldrick, *Acta Crystallogr., Sect. A: Found. Crystallogr.*, 2008, **64**, 112.
- 44 A. C. Sousa, M. C. Oliveira, L. O. Martins and M. P. Robalo, *Green Chem.*, 2014, **16**, 4127.
- 45 M. Shyamal, T. K. Mandal, A. Panja and A. Saha, *RSC Adv.*, 2014, **4**, 53520.
- 46 A. Hazari, L. K. Das, A. Bauzá, A. Frontera and A. Ghosh, *Dalton Trans.*, 2016, **45**, 5730.
- 47 A. Panja, M. Shyamal, A. Saha and T. K. Mandal, *Dalton Trans.*, 2014, **43**, 5443.
- 48 A. Panja, *Dalton Trans.*, 2014, **43**, 7760.
- 49 L. Mandal and S. Mohanta, *Dalton Trans.*, 2014, **43**, 15737.
- 50 H. Mori, N. Sakurai, S. Tanaka, H. Moriyama, T. Mori, H. Kobayashi and A. Kobayashi, *Chem. Mater.*, 2000, **12**, 2984.
- 51 S. Sen, P. Talukder, S. K. Dey, S. Mitra, G. Rosair, D. L. Hughes, G. P. A. Yap, G. Pilet, V. Gramlich and T. Matsushita, *Dalton Trans.*, 2006, 1758.
- 52 A. Ray, G. M. Rosair, R. Kadam and S. Mitra, *Polyhedron*, 2009, **28**, 796.
- 53 N. Sarkar, K. Harms, A. Bauzá, A. Frontera and S. Chattopadhyay, *ChemistrySelect*, 2017, **2**, 2975.
- 54 K. Ghosh, K. Harms and S. Chattopadhyay, *Polyhedron*, 2016, **112**, 6.
- 55 A. Panja, N. C. Jana, M. Patra, P. Brandão, C. E. Moore, D. M. Eichhorn and A. Frontera, *J. Mol. Catal. A: Chem.*, 2016, **412**, 56.